coatings

MDPI

Article

Evaluation of the Ultraviolet-Curing Kinetics of Ultraviolet-Polymerized Oligomers Cured Using Poly (Ethylene Glycol) Dimethacrylate

Ji-Won Park [1,2], Jong-Gyu Lee [1], Gyu-Seong Shim [1], Hyun-Joong Kim [1,2,*], Young-Kwan Kim [3], Sang-Eun Moon [3] and Dong-Hun No [3]

1 Program in Environmental Materials Science, College of Agriculture & Life Sciences, Seoul National University, Seoul 08826, Korea; roorouny@gmail.com (J.-W.P.); spdh123@snu.ac.kr (J.-G.L); sks6567@snu.ac.kr (G.-S.S.)
2 Research Institute of Agriculture and Life Sciences, Seoul National University, Seoul 08826, Korea
3 Samsung Display, Asan-si, Chungcheongnam-do 31454, Korea; ykwan13.kim@samsung.com (Y.-K.K.); se.moon@samsung.com (S.-E.M.); donghun.no@samsung.com (D.-H.N.)
* Correspondence: hjokim@snu.ac.kr; Tel.: +82-2-880-4784

Received: 27 January 2018; Accepted: 6 March 2018; Published: 9 March 2018

Abstract: Ultraviolet (UV)-curable oligomers are increasingly being used in various industries because they can be applied rapidly and have excellent physical properties. Ultraviolet polymerization is used for manufacturing such oligomers. Reactive diluents, which are employed during the secondary curing of UV-curable oligomers, can help elucidate the curing behaviors of these oligomers. In this study, poly (ethylene glycol) dimethacrylate (PEGDMA) was used as the reactive diluent for UV-curable oligomers. Photodifferential scanning calorimetry (photo-DSC) and shrinkage measurements revealed that the curing behavior of the polymers was dependent on the size and number of molecules of PEGDMA. The effect of the small-size PEGDMA on curing behavior was greater than that of the larger molecules. Further, in most cases, the use of a larger amount of PEGDMA resulted in lower reactivity.

Keywords: UV-curable oligomer; UV polymerization; UV-curing behavior; photo-DSC; shrinkage

1. Introduction

Ultraviolet (UV)-curable systems have several advantages such as rapid curing, low concentration of volatile organic compounds, and material diversity. Owing to these advantages, UV-curable systems are used in various industries, especially in the coating industry. UV-curable systems can also be used to implement solvent-free curing systems that consist of reactive diluents, polyfunctional oligomers, photoinitiators, and additives. Given the broad range of potentially usable materials, it is possible to construct a system suitable for various applications [1,2].

Solvent polymerization, which is popularly used in the industry, allows for a wide choice of solvents; therefore, the process conditions can be appropriately varied in order to tune the performance of the polymerized material. However, growing environmental concerns related to the use of these solvents has triggered the need for a solvent-free polymerization process [3–5].

Bulk polymerization is the simplest form of polymerization, but it has several disadvantages. For instance, it requires control of the heat generated as well as the molecular weight of the formed polymer, so this approach is rarely taken. To overcome these drawbacks, UV curing has been employed to control the heat generated and the polymerization time, thereby controlling the molecular structure. It is possible to produce a high-performance coating/adhesive oligomer system through secondary blending and a curing process [6,7].

In the preparation of oligomers, UV radiation is used in both polymerization and curing processes. The secondary curing process determines the physical properties of the oligomer. Important curing parameters include the curing rate and the shrinkage ratio. The curing rate has a significant effect on processability. Further, when the shrinkage ratio is high, the reliability of the oligomer decreases. Therefore, an analysis of these curing parameters is essential. These parameters are dependent on the reactive diluent used for the secondary curing process. Care should be taken when choosing the appropriate diluent, as it determines not only the curing properties but also the viscosity and specific characteristics of the oligomer [8–10].

UV curing is controlled by various variables. Therefore, it is very important to evaluate the UV curing behavior. UV curing behavior analysis for single materials has been carried out. Photo-DSC can calculate the instantaneous reaction rate by checking the calorific value of the material in real time. This can be used to evaluate the curing behavior of the material depending on its reactivity and environmental conditions [11–13]. Studies have also been conducted to calculate the amount of C=C depletion by observing the change in C=C double bonds peaks very rapidly using real-time FT-IR [14,15]. Recently, various studies have been made to analyze the shrinkage phenomenon occurring in the UV curing process [16,17].

UV curing properties for reactive diluents have been studied in a variety of environments and methods. However, studies on the binary structure of UV polymerization system and diluent are weak. This is because the interpretation of the UV curing behavior due to multiple influences is essential for the actual application of the final product [18,19].

In this study, the secondary curing behaviors of oligomers synthesized via UV-curing-based bulk polymerization were evaluated. In particular, the effects of the influencing factors related to the reactive diluent used were analyzed. The UV-curing behavior was determined based on the shrinkage during photodifferential scanning calorimetry (photo-DSC), and its relevance of complementary role between the shrinkage and photo-DSC was elucidated.

2. Materials and Methods

2.1. Preparation of UV-Curable Oligomers

UV-curable oligomers prepared by bulk polymerization underwent the stages shown in Figure 1. During the primary polymerization, the monomers and photoinitiators were added to the polymerization bottle, and the viscosity of the mixture was increased through a short UV-based polymerization. Then, the initiator and reactive diluents were added, and secondary curing progressed after a coating was formed on the surface of the final product or release film. The monomers used in the primary polymerization determined the properties of the final oligomer, while the reactive diluents used during the secondary curing stage significantly affected the curing properties [3,20,21].

In this study, 2-ethylhexyl acrylate (2-EHA, Sigma Aldrich, MO, USA), isobornyl acrylate (IBA; Sigma Aldrich, MO, USA), and N-vinyl caprolactam (NVC; Tokyo Chemical Industry, Tokyo, Japan) were used as the monomers without purification. Hydroxydimethyl acetophenone (Micure HP-8, Miwon Specialty Chemical, Yongin-si, Korea) was used as the photoinitiator. The main absorption ranges were 265–280 nm and 320–335 nm. The components were added in a ratio 2-EHA/IBA/NVC = 60:35:5 (weight fraction), while the photoinitiator was added in a total monomer ratio of 1 part per hundred resin (phr).

Polymerization was performed in a 500 mL four-necked round-bottomed flask equipped with a mechanical stirrer, an N_2 inlet, a thermometer, and an optical fiber of a UV lamp, as shown in Figure 2. The equipment used for polymerization is Spot-Cure (SP-9, USHIO, Tokyo, Japan). The UV lamp used mercury vapor, and the output was 250 W. The major wavelength was 280–320/365 nm. The temperature was maintained at room temperature, and the chemicals were subjected to constant stirring at 100 rpm. After being purged with N_2 for 30 min under constant stirring, the monomer mixtures were exposed to the UV lamp (20 mW/cm^2) for 70 s at room temperature under a flow of

N_2. The conversion rate of the primary polymerized polymer was measured to be approximately 20%. The primary polymerized material is called the "prepolymer." The molecular weights of the prepolymers were measured using a gas permeation chromatography (GPC) system (YL9100 GPC System, YoungLin Instruments, Anyang-si, Korea) equipped with a refractive index detector (YL9170, YoungLin Instruments). The GPC columns were eluted with tetrahydrofuran as the eluent solvent at 35 °C at a flow rate of 1 mL/min. The number-average (M_n) and weight-average (M_w) molecular weights were calculated using a calibration curve for polystyrene as the standard.

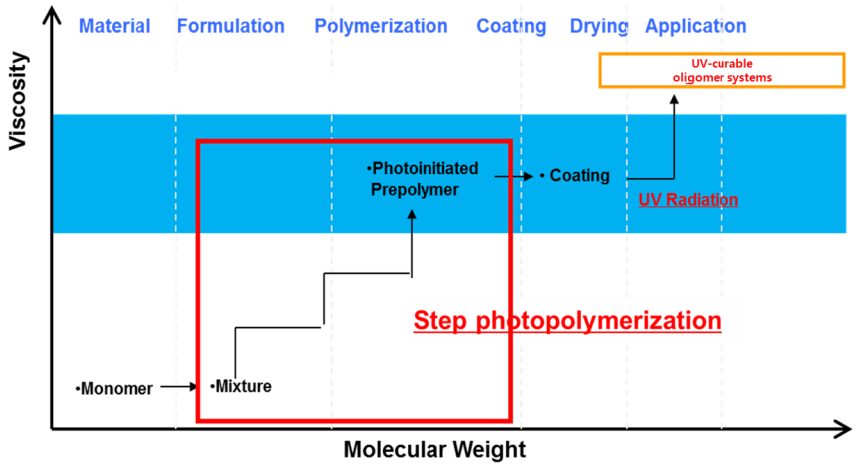

Figure 1. Status of ultraviolet (UV)-polymerized oligomers during various stages of the polymerization process.

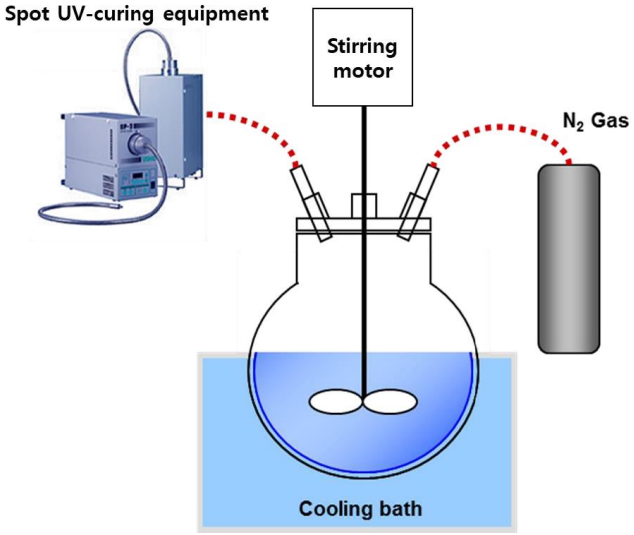

Figure 2. Equipment used for UV-curing-based polymerization.

Poly (ethylene glycol) dimethacrylate (PEGDMA; Sartomer, Colombes, France) was used as the reactive diluent for the secondary curing process. PEGDMA can be classified into the following grades depending on the size of the intermediate molecule: 100, 200, 400, and 1000. HP-8 was used as the photoinitiator in a concentration of 1 phr.

2.2. Evaluation of UV-Curing Behavior

Acrylate-based UV-curable materials undergo a growth reaction via a chain reaction upon exposure to light. In this case, the C=C carbon double bond formed single-stranded chains that released

energy. The amount of energy emitted was measured by photo-DSC, which was performed using a DSC Q-200 system with a photocalorimetric attachment (Photo-DSC, TA Instruments, New Castle, DE, USA). The light source was Spot-Cure (Omnicure-s2000, Excelitas, Waltham, MA, USA). Spot-Cure (Omnicure-s2000) uses a 200 W high-pressure mercury vapor lamp. Equipment of the same lamp type was selected to set the same test conditions. The intensity of the UV light used was determined by placing an empty DSC pan on the sample cell. The UV light intensity on the sample was 10 mW/cm^2 for wavelengths of 300–545 nm. The weight of the sample used was approximately 3 mg, and the sample was placed in an open aluminum DSC pan. The measurements were carried out at 25 °C.

2.3. Shrinkage Test

Controlling the shrinkage is the most important aspect of synthesizing UV-curable materials, as these materials shrink rapidly during the curing process, with the theoretical shrinkage rate being more than 20% [17]. This phenomenon of shrinkage can induce warpage in the material and generate internal stress, which can lead to defects in the finished product.

Most polymers will shrink continually in a direction-independent manner during curing, and it is extremely difficult to measure their volume. This shrinkage phenomenon depends on several internal and external factors. Linear shrinkage can be measured through a change in the length, as explained by the following equation. Based on the equation below, the linear shrinkage is equivalent to one-third of the volumetric shrinkage [22]:

$$\begin{aligned} &\text{Volume of Original Cubic (Edge length is } X) = X^3 \\ &\text{Volume of Original Cubic (Edge length is } X) = X^3 \\ &\text{Volume of Shrinkage Cubic (Edge length is } X - a,\ a \text{ is linear shrinkage ratio)} \\ &= (X-a)^3 \\ &= X^3 - 3aX^2 + 3a^2X - a^3 \ (a \text{ is small, so we can ignore } a^2 \text{ and } a^3) \\ &= a^2(X - 3a) \end{aligned} \quad (1)$$

On the other hand, Lee and Park demonstrated that the linear shrinkage and volumetric shrinkage can be similar, depending on the experimental conditions. In particular, when the aspect ratio of the material in question is high, the linear shrinkage is very similar to the volumetric shrinkage [17,23].

In this study, the shrinkage ratio was measured using a linometer (RB Model 308, R&B, Daejeon, Korea). The light source was Spot-Cure (SP-9), which utilized the same equipment used in the UV polymerization process. The output of the light source was adjusted to 10 mW/cm^2. First, a sample of the polymer to be tested was loaded onto a stainless steel plate and covered with a glass slide. These were then placed on a linear variable differential transformer, and a glass slide was placed on top [16,23]. As the sample shrank under UV irradiation, the stainless steel plate moved, and the movement distance was recorded. This linear shrinkage in the vertical direction was transformed into volumetric data, and the shrinkage ratio was calculated [8].

3. Results and Discussion

3.1. Evaluation of the Molecular-Weight Distribution of the Prepolymer

Figure 3 shows the molecular weights of the prepolymer used. Unlike conventional polymers, this prepolymer exhibited very specific molecular weight distributions. Table 1 shows the M_n and M_w values of three sections (at Figure 3a–c) of the prepolymer molecular weight. In Figure 3a, an oligomer with a high molecular weight can be identified. The figure suggests the presence of a polymer with a number-average molecular weight of 600,000 g/mol or higher and a weight-average molecular weight of 1.5 million g/mol or higher. The polydispersity index (PDI) is 2.35, which is not large. In this photopolymerization system, the molecular weight in the polymer region is high, owing to which the viscosity was also very high. Figure 3b shows the sectional characteristics of the

photopolymerization system. The area ratio for the section shown is very large. During general solvent polymerization, it is the monomolecules in this section, such as those of a solvent, that are measured. The number-average/weight-average molecular weight corresponding to this section, which was related to a highly uniform material having a PDI of 1.03, was measured to be approximately 160 g/mol. Photopolymerization is characterized by bulk polymerization, which has a lower ratio of conversion than an increase in viscosity. As the reaction proceeds, various side reactions also occur, and the process eventually enters a state wherein polymerization can no longer occur. In general, the reaction time limit for the photopolymerization process depends on the composition of the system but is determined at a conversion ratio of approximately 20%–25% [24]. In this study, the conversion rate was tracked through FT-IR. Thus, the prepolymer continues to constitute a very high proportion of the monomer. It can be assumed that Figure 3b shows the molecular weights of 2-EHA and IBA, which are present in high proportions and have higher molecular weights as compared to those of the monomers used in the reaction. The section shown in Figure 3c has a relatively lower molecular weight as compared to that shown in Figure 3b and can be interpreted as a molecular section of NVC, which has a relatively smaller molecular size and a ring structure as well as a small volume. Photopolymerization systems contain a large number of single molecules distributed in this manner, so it is necessary to use polyfunctional oligomers.

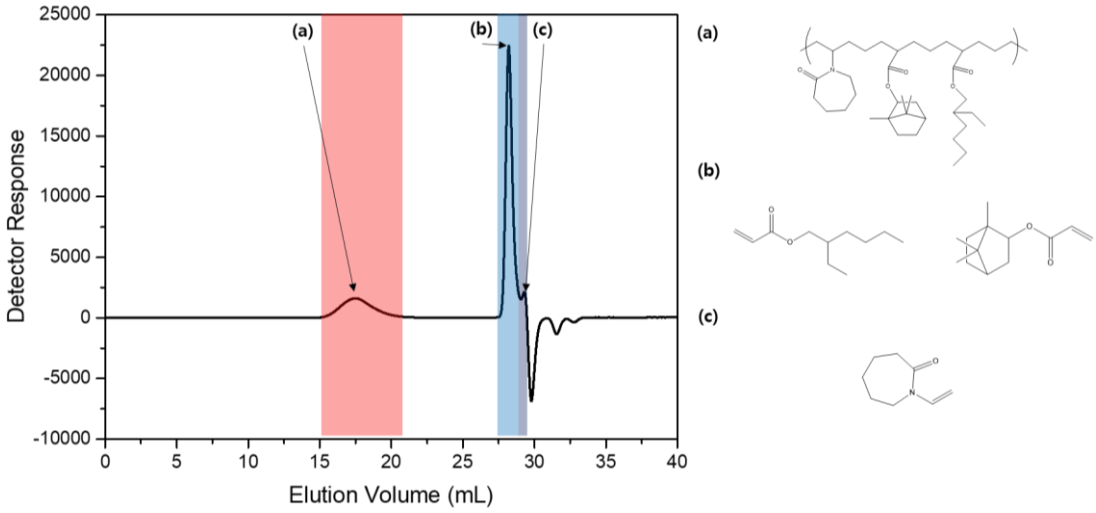

Figure 3. Molecular weights of the prepolymer as determined using gas permeation chromatography (GPC): (**a**) the polymer-forming section, (**b**) the section corresponding to 2-EHA/IBA, and (**c**) the section corresponding to N-vinyl caprolactam (NVC).

Table 1. Molecular weight distribution of the prepolymer.

Section	M_n	M_w	PDI
A	637,990	1,504,900	2.358
B	156	161	1.032
C	67	68	1.005

3.2. Evaluation of UV-Curing Behavior Using Photo-DSC

Figure 4 shows the results of the photo-DSC measurements performed on the UV-curable system using poly (ethylene glycol) dimethacrylate with an intermediate molecule size of 100 (PEGDMA100). The graphs show the changes in the peak approach time and the maximum heat flow. The peak of heat flow decreased as the PEGDMA content was increased. At the same time, the peak approach time increased continuously. Thus, the results of the photo -DSC measurements were in keeping with the expectations. As the PEGDMA size was increased, the heat flow peak became broader. That is to say,

a phenomenon similar to the merging of two reaction peaks occurred. Methacrylate is generally less reactive than acrylate. While acrylate forms secondary radicals, methacrylate forms tertiary radicals, which are more stable and less reactive. The steric effect of the "metha" structure is also a major factor in reducing the reaction rate. This structure also influences the overall structure by changing the r1-r1/r1-r2 response.

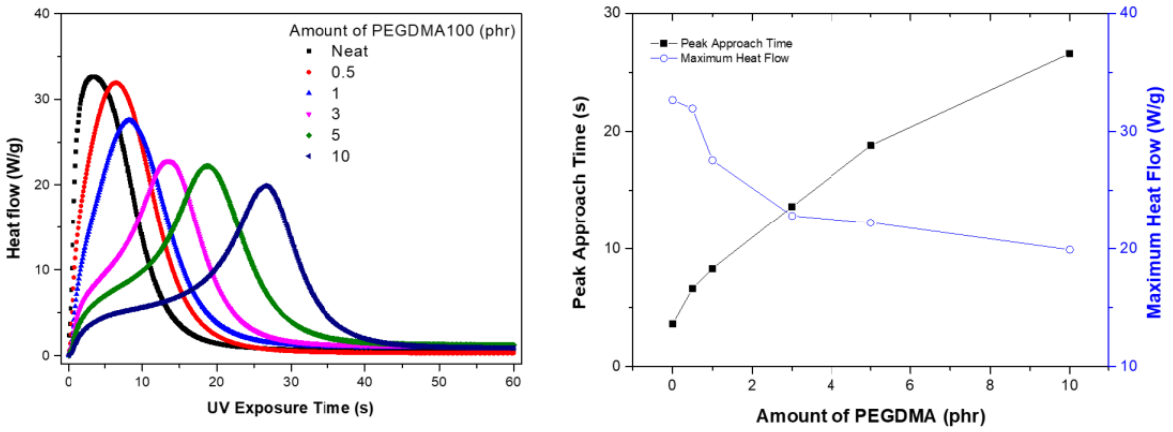

(**a**) (**b**)

Figure 4. Photodifferential scanning calorimetry (photo-DSC) results for a UV-curing system obtained using poly (ethylene glycol) dimethacrylate with an intermediate molecule size of 100 (PEGDMA100): (**a**) real-time heat flow; (**b**) peak approach time and maximum heat flow.

In a mixed system consisting of an acrylate and a methacrylate, the reactivity varies dramatically with the mixing ratio. However, this change is not simply determined by the proportion of weight of the material. Figure 5 shows the results of photo-DSC measurements performed on the UV-curable system using PEGDMA with different molecular weights. As the molecular weight of PEGDMA increases, the rate of increase in the peak approach time decreases. When the molecular weight of the core structure of PEGDMA is 1000 g/mol, the change in the approach time is very small even though the content increases to 10 phr. It was also confirmed that the rate of decrease of the peak of heat flow is the smallest when the molecular weight of PEGDMA is the highest. Increasing the molecular weight of PEGDMA implies that the functionality number of methacrylate is reduced.

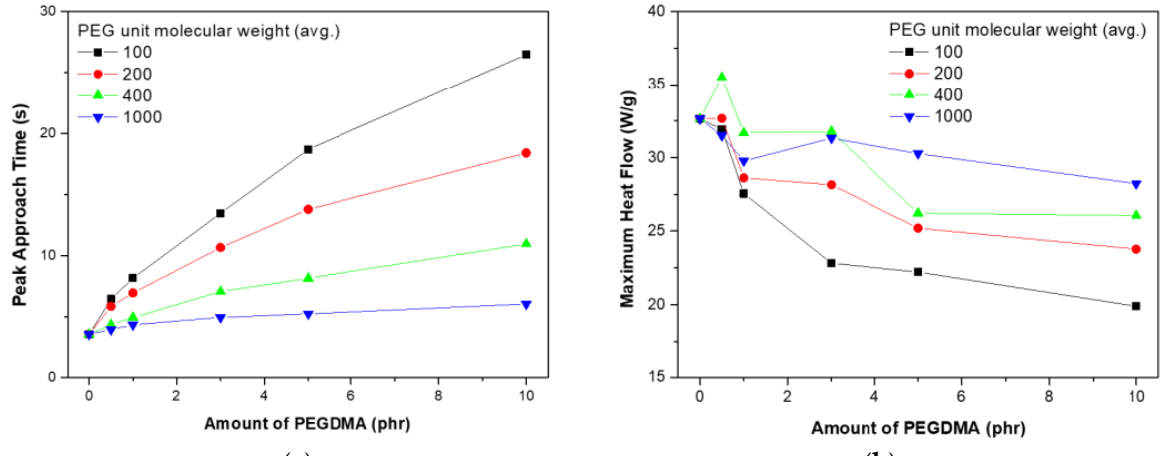

(**a**) (**b**)

Figure 5. Change in reactivity with size of poly (ethylene glycol) dimethacrylate (PEGDMA) as determined using photo-DSC: (**a**) peak approach time; (**b**) maximum heat flow.

When the PEG unit is small, the proportion of the functional groups on the methacrylate structure increases sharply. The more functional groups there are on the structure, the lower the molecular weight is. The molecular weights of PEGDMA with the PEG units of 100, 200, 400, and 1000 are approximately 250, 350, 550, and 1150, respectively. The methacrylate proportion of the mixture system was calculated based on these molecular weights. The highest proportion—PEG unit 100/10 phr—was set as Reference Point 1, and the reverse rate was calculated. The peak time for each relative value is displayed in Figure 6. A linearly increasing tendency was observed with the increase in the proportion of the methacrylate structure. The correlation between the time and the proportion of the methacrylate structure was analyzed by linear regression analysis of the model given below:

$$Y = \beta_0 + \beta_1 x_1 + \beta_2 x_2 \ldots + \beta_p x_p \quad (2)$$

β_n is the coefficient of the independent variable and x_n is the explanatory variable. It can be seen that there is a very high level of correlation, with the R^2 value being 0.966. Consequently, the delay effect of the methacrylate structure on the UV-curing reaction is highly linear. Thus, it can be assumed that the material can be controlled based on this characteristic using an acrylate and a methacrylate, because they allow for the control of the reaction rate.

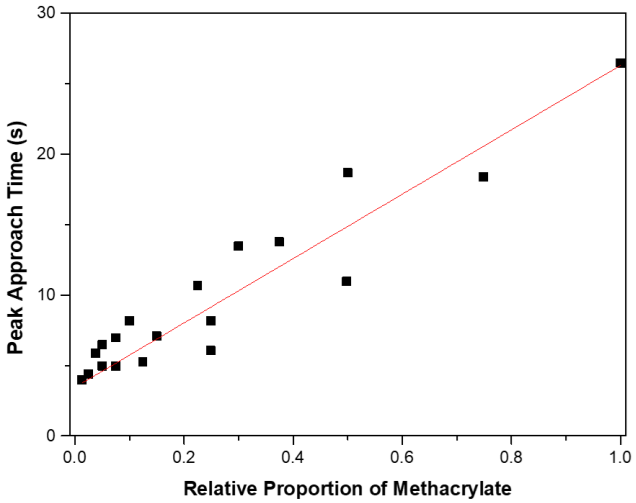

Figure 6. Change in peak approach time with changes in relative proportion of methacrylate (R^2 = 0.966).

Acrylate and methacrylate have a large difference in reaction rate. This difference in reaction rates does not directly affect the final conversion rate. The final conversion rate is an important factor because it affects the stability of the material. Methacrylate is slow but the final conversion rate is even higher. In the course of the reaction, a continuous reaction is possible by the mobility of the molecule by the "metha" structure [22].

The peak approach time represents the rate of growth and can be employed as an indicator of how fast the chain reaction is in the case of the material reaction initiated by UV curing. Because the structure of the diluent is that of a methacrylate, the reaction rate is low as compared to that of the prepolymer. The reactivity gap between the acrylate and the methacrylate is large in most UV-curable systems [24]. Figure 7 shows the total reaction heat (exothermic area) of the system as determined using PEGDMA100. Based on the results of photo-DSC, the exothermic area was calculated; this was reflective of the total heat flow. The exothermic area was determined to be larger than the neat area for all conditions. The reaction rate of the methacrylate structure was low. However, the structure contained molecules that induced the overall reaction by creating a bridge in the middle. Therefore, the total heat of reaction was higher compared to that in the case of the neat prepolymer.

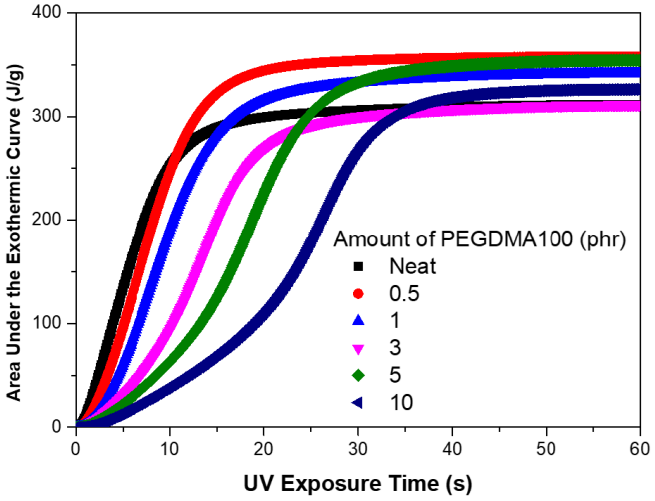

Figure 7. Total heat flow (area under the exothermic curve) of a UV-curing system based on PEGDMA100.

Figure 8 shows the results of photo-DSC for different molecular sizes of PEGDMA. Each data point corresponds to a content of 10 phr. As the molecular weight of PEGDMA is increased, the graph becomes similar to that for the neat prepolymer. Thus, when the molecular weight is low, the structure acts as a bridge within the prepolymer. However, when the molecular weight is high, it behaves like the prepolymer. According to previous research, the actual conversion rate does not reach the theoretical value when the curing process has progressed considerably. Park (2003) explained that the caging of the material causes this phenomenon. It is possible to interpret the results for this system in a similar manner. That is to say, aggregated islands of the diluent are formed when the proportion of the diluent is increased, leading to the generation of a diluent-caged zone. In addition, the prepolymer is dispersed, and the acrylate population is decreased. It has been stated that the caged zone forms for a variety of reasons. Polymer growth occurs in a partial manner. A part of the growth zone forms in the early stage as T_g increases, causing a reduction in the mobility of the molecules. Because the number of functional groups decreases with an increase in the PEG unit content, a greater reduction in the reactivity can be expected. However, the actual reduction rate is not very high. The reason is that the PEG units are more flexible in a longer molecular structure. Hence, as described above, the effect of T_g on the reaction progress is weakened as well [22,25].

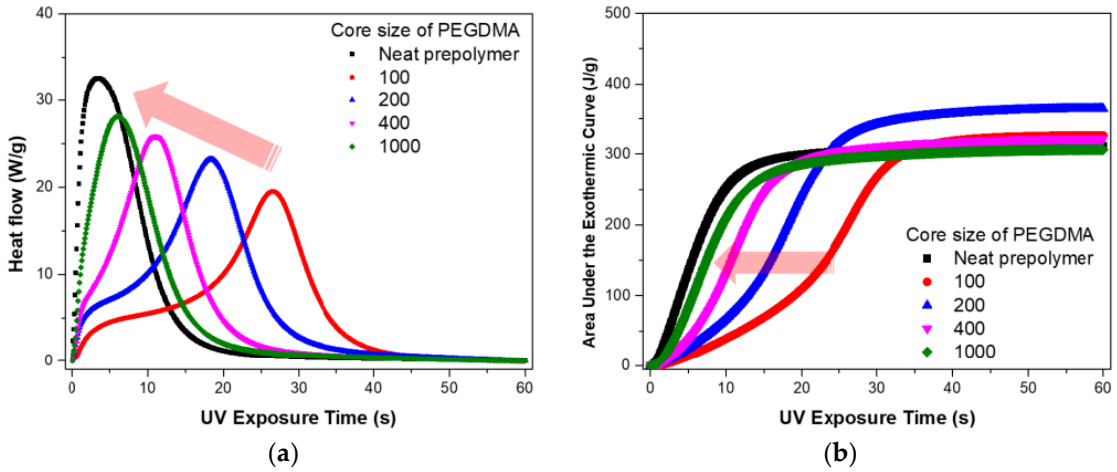

Figure 8. Reactivity for different PEGDMA sizes as determined using photo-DSC for a concentration of 10 phr: (**a**) peak heat flow; (**b**) total heat flow.

3.3. Shrinkage Rest

The results of the shrinkage ratio measurements are shown in Figure 9. The shrinkage ratio can be used as an indicator of the degree of curing of the entire material. The shrinkage phenomenon, in contrast to the photo-DSC measurements, does not occur immediately upon exposure to UV radiation. The initial measurement of the curing does not proceed, as shown in Figure 10. The entire network is formed in this manner. Thus, there is a delay in the interpretation of the results as well as the evaluation of the peak time for the photo-DSC measurements. These properties can be used as an indicator to evaluate the bulk properties of the material. Park et al. [17] explained that a depth profile of UV-curable systems can be obtained based on this phenomenon. The time taken by the UV radiation to penetrate from the surface to the core can be measured, and this parameter has been used to analyze the surface UV-absorption effect of the UV-curable system [26].

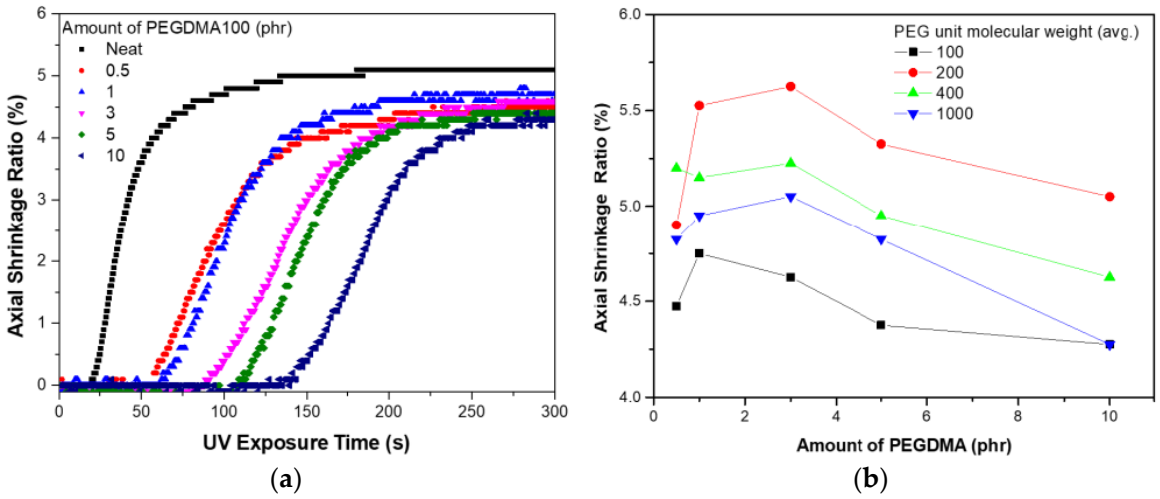

Figure 9. Shrinkage ratio of a UV-curable system (**a**) when using PEGDMA100 and (**b**) for different PEGDMA sizes.

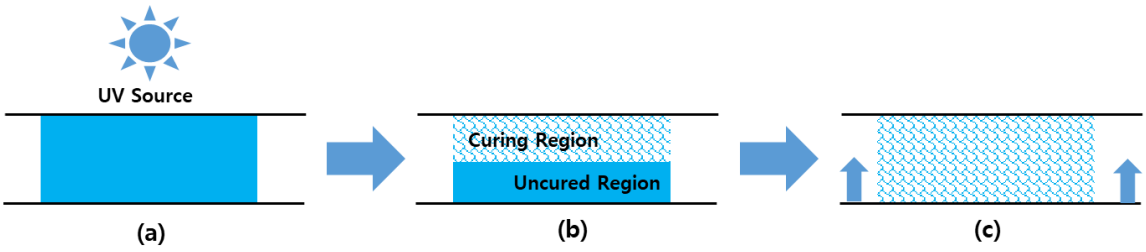

Figure 10. The shrinkage measurement process: (**a**) exposure to light source, (**b**) surface curing/no curing within material (no shrinkage measured), and (**c**) deep curing (start of shrinkage measurement).

As the content of PEGDMA is increased, the shrinkage rate tends to decrease. This tendency is due to the difference in the shrinkage ratios of the two materials. Generally, acrylate shrinks more than methacrylate having the same structure. However, these differences have different effects, depending on the core structure. The packing and conformation of the molecular structure both affect the shrinkage phenomenon [26]. When the size of the PEGDMA core is 200, the shrinkage rate tends to be relatively higher. A nanopore-related effect can be expected when materials with different molecular weights are mixed. When the PEGDMA core size is 100, the molecular weight is 200, which is similar to the size of the acrylate. Therefore, the molecular size has no effect in this case. As the core size is increased, the effect of the difference in molecular size increases. However, if the molecular weight is too large, the shrinkage ratio becomes relatively smaller. This is because the flexibility of the chain

increases, and the number of reactive contacts decreases. The decrease in the width due to shrinkage for common UV-curable oligomers is approximately 2%–3%. Further, a difference of more than 1% is considered a large one, and controlling this shrinkage would have a major impact on the properties of the final material, such as the internal stress and the rainbow effect [17].

The shrinkage ratio is an indexical numerical value that reflects the conversion rate of a material. The conversion and reaction rates exhibit a relationship that can be expressed through integration and differentiation; the exothermic area is calculated by integrating the photo-DSC curve, while the shrinkage rate can be calculated by differentiating the shrinkage ratio. Figure 11 shows the results of the differentiation of the shrinkage ratio, which is represented as the reaction rate. The curve is similar to that obtained from the photo-DSC measurements. It is clear that the phenomenon of delayed shrinkage is in accordance with the PEGDMA content. However, shrinkage is a phenomenon that occurs in the bulk structure, as opposed to those that occur during the photo-DSC measurements. Further, because the photo-DSC process is subject to various influences, a linear relationship does not exist. The shrinkage ratio increases owing to structural factors such as the conformation when the polymer has a larger molecular size. In this case, the shrinkage degree is very high, and the structure of a chain number of reaction occurs for the same reaction time. When a more extensive methacrylate structure exists, the reaction rate is lowered, and the shrinkage phenomenon of the entire structure is delayed as well. Figure 12 shows the peak approach time and shrinkage rate as determined through the shrinkage measurements. While these results are in keeping with those of the photo-DSC analysis, they are not an exact match. However, they indicate that the bulk properties can be used to examine the curing behavior of the molecules. Based on these results, it can be concluded that photo-DSC and shrinkage measurements can be used together as complementary techniques for analyzing the curing behaviors of UV-curable oligomers.

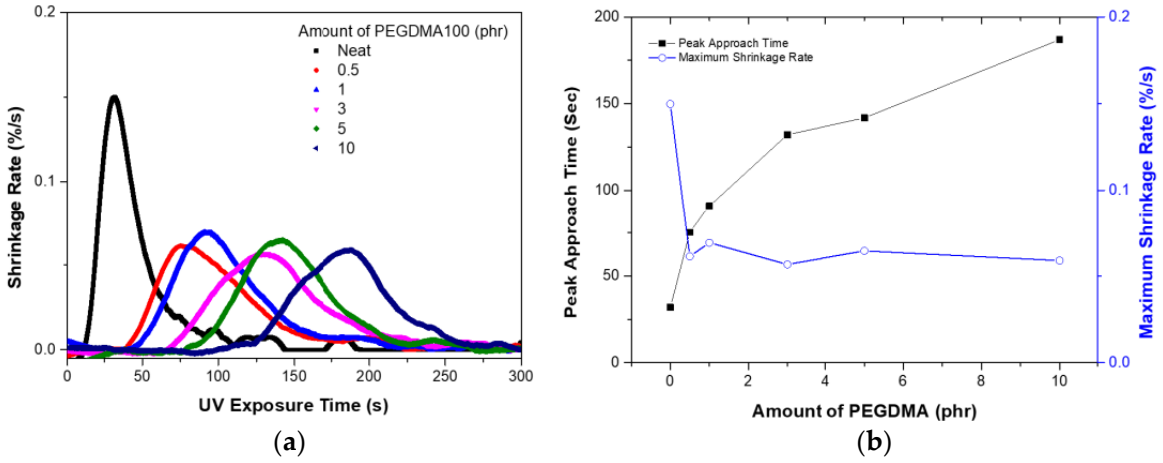

Figure 11. Analysis of shrinkage rate of a UV-curable system using PEGDMA100: (**a**) shrinkage rate; (**b**) peak approach time and maximum shrinkage rate.

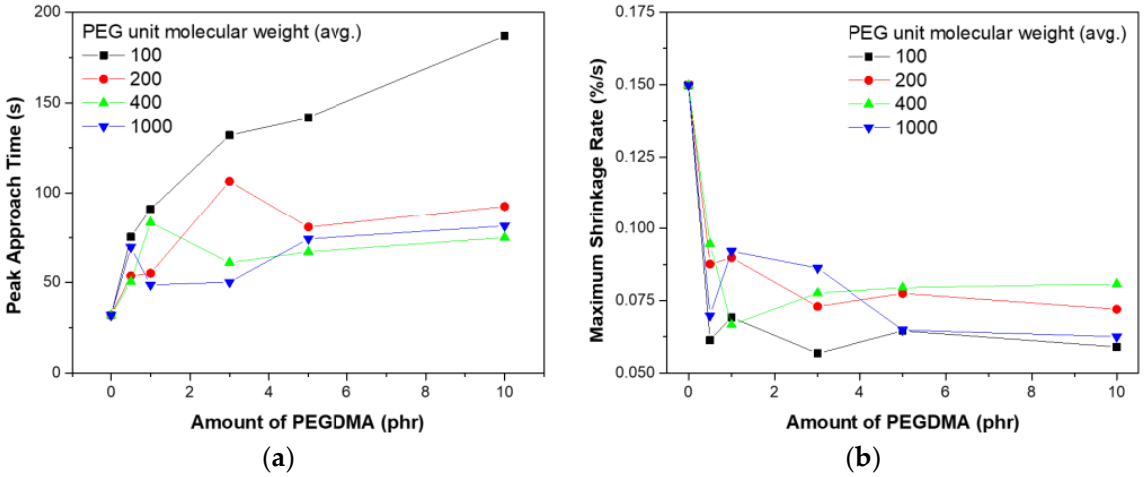

Figure 12. Shrinkage rates for different PEGDMA sizes: (**a**) peak approach time; (**b**) maximum shrinkage rate.

4. Conclusions

The UV polymerization process was used to produce a prepolymer containing a polymer, an oligomer, and a monomer. The prepolymer had a molecular weight of more than 1 million g/mol, which is much larger than that of a general acrylate polymer and had a very broad molecular weight distribution. The UV-curing behavior of UV-curable oligomers varied with the size and content of the diluent used. When using a small-molecular-weight diluent, the polymerization reaction was delayed, and the change in the reaction rate was large. The reaction delay was linearly related to the proportion of the methacrylate structure within the overall structure. It was confirmed that the reaction rate can be controlled using a diluent having a "metha" structure. In particular, since the overall reactive rate can be slowed down and the conversion rate can be maintained at a similar level, it is considered easy to control the speed according to the system. The shrinkage phenomenon is similar to general UV-curing behavior. Based on the relationship between the UV-curing behavior and the shrinkage phenomenon, it was possible to elucidate their complementary nature. In addition to the previously evaluated variables, several other factors also affected the curing process. Based on a multilateral examination of these factors, it is believed that the curing characteristics of UV-curable oligomers can be predicted with greater accuracy.

Acknowledgments: This study was supported by the Samsung Display Corporation.

Author Contributions: Ji-Won Park and Hyun-Joong Kim conceived and designed the experiments; Jong-Gyu Lee, Young-Kwan Kim and Sang-Eun Moon performed the experiments; Gyu-Seong Shim and Ji-Won Park analyzed the data; Dong-Hun No contributed reagents/materials/analysis tools; Ji-Won Park wrote the paper.

Conflicts of Interest: The authors declare no conflict of interest.

References

1. Maag, K.; Lenhard, W.; Löffles, H. New UV curing systems for automotive applications. *Prog. Org. Coat.* **2000**, *40*, 93–97. [CrossRef]
2. Yao, M.; Wang, R.-m.; Dong, M. Research progress of UV curing system. *China Adhes.* **2006**, *15*, 33.
3. Kajtna, J.; Krajnc, M. Solventless uv crosslinkable acrylic pressure sensitive adhesives. *Int. J. Adhes. Adhes.* **2011**, *31*, 822–831. [CrossRef]
4. Fukui, H.; Ishizawa, H.; Nakasuga, A. Development of photo-curable pressure sensitive adhesives with UV cationic curing of epoxy resins. *J. Photopolym. Sci. Technol.* **1999**, *12*, 169–172. [CrossRef]
5. Decker, C.; Viet, T.N.T.; Decker, D.; Weber-Koehl, E. UV-radiation curing of acrylate/epoxide systems. *Polymer* **2001**, *42*, 5531–5541. [CrossRef]

6. Crivello, J.V.; Reichmanis, E. Photopolymer materials and processes for advanced technologies. *Chem. Mater.* **2013**, *26*, 533–548. [CrossRef]
7. Decker, C. The use of UV irradiation in polymerization. *Polym. Int.* **1998**, *45*, 133–141. [CrossRef]
8. Garoushi, S.; Vallittu, P.K.; Watts, D.C.; Lassila, L.V. Polymerization shrinkage of experimental short glass fiber-reinforced composite with semi-inter penetrating polymer network matrix. *Dent. Mater.* **2008**, *24*, 211–215. [CrossRef] [PubMed]
9. Wang, Q.K.; Huang, B.Q.; Wei, X.F.; Shen, H.C. Study on Shrinkage of Cured Volume for UV-Curing Coatings. In *Applied Mechanics and Materials*; Trans Tech Publ: Zürich, Switzerland, 2015; pp. 588–592.
10. Lee, S.-W.; Park, J.-W.; Park, C.-H.; Kwon, Y.-E.; Kim, H.-J.; Kim, E.-A.; Woo, H.-S.; Schwartz, S.; Rafailovich, M.; Sokolov, J. Optical properties and uv-curing behaviors of optically clear PSA-TiO2 nano-composites. *Int. J. Adhes. Adhes.* **2013**, *44*, 200–208. [CrossRef]
11. Scott, T.F.; Cook, W.D.; Forsythe, J.S. Photo-DSC cure kinetics of vinyl ester resins. I. Influence of temperature. *Polymer* **2002**, *43*, 5839–5845. [CrossRef]
12. Esen, D.S.; Karasu, F.; Arsu, N. The investigation of photoinitiated polymerization of multifunctional acrylates with TX-BT by photo-DSC and RT-FTIR. *Prog. Org. Coat.* **2011**, *70*, 102–107. [CrossRef]
13. Cho, J.-D.; Hong, J.-W. Photo-curing kinetics for the UV-initiated cationic polymerization of a cycloaliphatic diepoxide system photosensitized by thioxanthone. *Eur. Polym. J.* **2005**, *41*, 367–374. [CrossRef]
14. Scherzer, T.; Tauber, A.; Mehnert, R. UV curing of pressure sensitive adhesives studied by real-time ftir-atr spectroscopy. *Vib. Spectrosc.* **2002**, *29*, 125–131. [CrossRef]
15. Scherzer, T. Depth profiling of the conversion during the photopolymerization of acrylates using real-time ftir-atr spectroscopy. *Vib. Spectrosc.* **2002**, *29*, 139–145. [CrossRef]
16. Alvarez-Gayosso, C.; Barceló-Santana, F.; Guerrero-Ibarra, J.; Sáez-Espínola, G.; Canseco-Martínez, M.A. Calculation of contraction rates due to shrinkage in light-cured composites. *Dent. Mater.* **2004**, *20*, 228–235. [CrossRef]
17. Park, J.-W.; Shim, G.-S.; Back, J.-H.; Kim, H.-J.; Shin, S.; Hwang, T.-S. Characteristic shrinkage evaluation of photocurable materials. *Polym. Test.* **2016**, *56*, 344–353. [CrossRef]
18. Lee, J.-G.; Shim, G.-S.; Park, J.-W.; Kim, H.-J.; Han, K.-Y. Kinetic and mechanical properties of dual curable adhesives for display bonding process. *Int. J. Adhes. Adhes.* **2016**, *70*, 249–259. [CrossRef]
19. Lee, J.-G.; Shim, G.-S.; Park, J.-W.; Kim, H.-J.; Moon, S.-E.; Kim, Y.-K.; No, D.-H.; Kim, J.-H.; Han, K.-Y. Curing behavior and viscoelasticity of dual-curable adhesives based on high-reactivity azo initiator. *J. Electron. Mater.* **2016**, *45*, 3786–3794. [CrossRef]
20. Do, H.-S.; Park, Y.-J.; Kim, H.-J. Preparation and adhesion performance of UV-crosslinkable acrylic pressure sensitive adhesives. *J. Adhes. Sci. Technol.* **2006**, *20*, 1529–1545. [CrossRef]
21. Chiang, T.H.; Hsieh, T.-E. A study of monomer's effect on adhesion strength of uv-curable resins. *Int. J. Adhes. Adhes.* **2006**, *26*, 520–531. [CrossRef]
22. Park, J.-W. *Evaluation of Curing Shrinkage of the Photo-Curable Material and Its Application for Photo-Curable Adhesives*; Seoul National University: Seoul, Korea, 2016.
23. Lee, I.-B.; Cho, B.-H.; Son, H.-H.; Um, C.-M.; Lim, B.-S. The effect of consistency, specimen geometry and adhesion on the axial polymerization shrinkage measurement of light cured composites. *Dent. Mater.* **2006**, *22*, 1071–1079. [CrossRef] [PubMed]
24. Park, J.-W. Evaluation of UV Curing Behavior of UV Curable Resin through a Variety of Devices. In Proceedings of the 5th China International Bonding & 5th Asian Conference on Adhesion, Beijing, China, 15–17 September 2013.
25. Moeck, A.; Ag, R. Shrinkage of UV Oligomers and Monomers. In Proceedings of the RadTech UV/EB 2014, Rosemont, IL, USA, 12–14 May 2014; pp. 5–9.
26. Narang, A.S.; Boddu, S.H. Excipient applications in formulation design and drug delivery. In *Excipient Applications in Formulation Design and Drug Delivery*; Springer: Berlin, Germany, 2015; pp. 1–10.